Pattern Recognition Letters 6 (1987) 303–313
North-Holland

December 1987

Feature detection from local energy

M.C. MORRONE and R.A. OWENS*

*Departments of Psychology and *Computer Science, University of Western Australia, Nedlands, WA 6009, Australia*

Received 6 April 1987

Abstract: A more general definition of features such as edges, shadows and bars is developed, based on an analysis of the phase of the harmonic components. These features always occur at points of maximum phase congruency, the type of feature depending on the value of the phase. Using the image itself and its Hilbert transform, a local energy function is defined and it is shown that the local maxima of this energy function occur at points of maximum phase congruency.

Key words: Edge detection, phase, Hilbert transform, odd and even symmetric filters, energy.

1. Introduction

It now seems to be universally agreed that edge detection is an essential part of the early processing in any visual system, be it biological or physical. But the exact definition of what is to be considered an edge, and how such a feature may be detected optimally, is still the subject of intense debate (Boie et al., 1986; Canny, 1983; Hildreth, 1985; Morrone et al., 1986). In most systems, an edge is modelled as a discontinuity in the intensity profile or in its first derivative, the first case being idealised by a step function, the second by a trapezoidal function. Edge detectors traditionally try to detect the point of discontinuity of the function, or the middle of the ramp in the case of the trapezoid.

The work of Marr (1980) was seminal to most edge detection schemes. He produced a computational model that was well supported by physiological evidence, yet is is difficult to implement his algorithm successfully for machine vision. To improve the signal to noise ratio and the localisation Marr's scheme needs to be implemented over a number of scales, possibly a continuum of scales to obtain a full fingerprint description of the edges (Yuille and Poggio, 1985).

Canny's (1983) approach produced several optimal convolution operators for the detection of step functions, trapezoids, and triangular waveforms. These operators were calculated subject to three performance constraints: maximum signal to noise ratio, optimum localisation, and a single response to a single edge. Whilst offering numerous advantages because of these constraints, Canny's techniques do not easily distinguish between different types of features, since the same feature can be marked by the different operators, and usually at different points.

One of the major problems common to both Marr's and Canny's algorithms, as well as all other edge detection schemes that use a differential approach, is that they suffer from the problem of 'false positives'; that is, some points of maximum gradient will be marked as edges when humans do not perceive them as such (Richter and Ullman, 1986). For example, no edge is perceived in a sine-wave grating at the point where the luminance crosses its mean value, that is, the point at which the gradient is maximum or the second derivative is zero.

Step, trapezoidal and sinusoidal functions are perceived quite differently by the human visual system, as can be seen in Figure 1. In the first case we see a sharp edge; in the second we have no exact notion of the location of the middle of the ramp but rather we perceive light and dark bands nearby

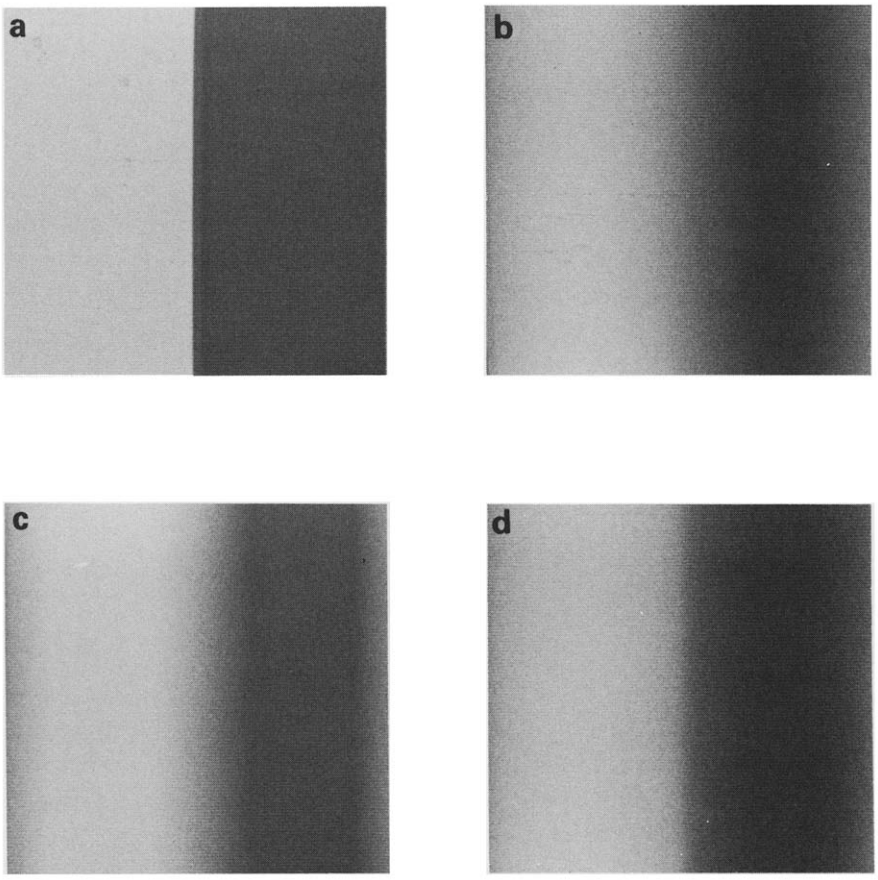

Figure 1. Four grating patterns illustrating different features. Their profiles are shown in Figure 3.

(a) A squarewave, producing an edge feature.

(b) A sinusoidal grating. No feature is perceived, only a smooth graduation of luminance.

(c) A tapezoidal waveform for which the ratio of the ramp width to the period is $t = 0.25$. Note the appearance of the sharp Mach bands where the ramp meets the plateau and that no edge is perceived. The formula of the luminance profile is given by:

$$\begin{aligned} F(x) &= 2Ax/tT, && 0 \le x \le tT/2, \\ &= A, && tT/2 \le x \le (T - tT)/2, \\ &= 2A\{(t/2) - x\}/tT, && (T - tT)/2 \le x \le T/2, \\ &= -F(-x), && -T/2 \le x \le 0, \end{aligned}$$

where A is the amplitude and T is the period. As t varies from 0 to 0.5, this family of functions ranges from a squarewave through to a triangular waveform.

The Fourier expansions of such functions about the origin are given by:

$$\sum_{k=0}^{\infty} [(4A/t\pi^2) \cdot (\sin(\pi t(2k+1))/(2k+1)^2)] \cdot \sin(2\pi(2k+1)x/T).$$

The amplitude spectra of these waveforms have only the odd terms non-zero, and these terms fall into alternately positively and negatively weighted blocks whose size varies inversely with t.

(d) An 'all positive trapezoid', produced by altering the Fourier expansion of the waveform in Figure 1c to force zero phase congruency at the origin. This pattern has the same amplitude spectra as the trapezoid in Figure 1c, but the Fourier coefficients are all positive. Note that an edge is perceived where 0^c phase congruency occurs.

the points of tangent discontinuities, known as Mach bands; we see the sine wave as a smooth, gradual luminance change with no obvious features. A step edge is typical of the sharp changes in luminance at the boundary between two objects (although not all edges are produced in this way);

and the trapezoid function models shadow edges in diffuse lighting, with the ramp representing the penumbra between the unshaded regions and the umbra.

Earlier work (Morrone et al., 1986) has suggested that the human visual system is capable of discriminating between a square waveform and a trapezoid by using phase information. The results of that paper indicate that the visual system perceives a positive-going edge at a point where all the harmonic components of the image spectrum cross zero with a positive slope, that is, at a point for which the phase of each component is zero.

This condition is clearly satisfied for the step function in Figure 1a at the transition point. The Fourier expansion of this function about the transition point contains only positive since components, all in zero phase. The same condition can be generated artificially as in Figure 1d. This waveform has only positive sine components, but the amplitude coefficients are derived from the expansion of a trapezoidal waveform. At the point where the phase of all the components is zero an edge is perceived, even though the profile of this function is continuous (see Figure 3d).

These ideas indicate that an edge could be defined more generally as any point at which all the spectral components have 0° phase. Analogously, a narrow bar could be defined as any point at which all the spectral components have 90° phase congruency, this being typical of a delta function.

Trapezoidal waveforms have blocks of negatively weighted harmonics which break the congruence of the phase at the point half-way through the ramp (see equation in caption of Figure 1c). No edge is perceived at this point. However, the periodic halt of the phase advance of the harmonics causes a phase congruency at the points where the ramps meet plateaux. The phase of the harmonic components of the trapezoid shown in Figure 1c alternates, at that point, between 45° and 135°. At all other points the phase values differ by more than 90°, e.g. at the point half-way through the ramp the phase sequence is {0°,0°,180°,180°,..}. Thus for a trapezoidal waveform the strongest phase congruency occurs at the points where the ramp meets the plateau and ideally these are the features that a detector should mark.

The aim of our work has been to construct an algorithm that detects points of strong phase congruency. Intuitively, a point of strong phase congruency should relate to a maximum in the energy of the waveform. Thus an important feature of our algorithm is the construction of a local energy function of the image. It is demonstrated that the maxima of the energy function occur at points of maximum phase congruency and these points are used to detect and localise features. An analysis of the type of phase congruency that generates maxima allows a distinction between different types of features, for example, edges, bars, etc. The results show that the algorithm is very robust to noise and does not mark false positives; for example, it has zero response everywhere to a sinewave.

2. Algorithm

To detect the points of phase congruency an energy function is defined. The energy of an image is extracted by using the standard method (see Gabor, 1946) of squaring the outputs of two filters that are 90° out of phase, i.e., that form a quadrature pair. For example (Adelson and Bergen, 1985), in the case of Gabor functions, a quadrature pair is formed by using the sine and cosine versions of the same filter. The following algorithm uses the image itself and its Hilbert transform. The Hilbert transform, although normally defined as an improper integral (see Titchmarsh, 1948), is related to the Fourier expansion of the image in that it has the same amplitude spectrum and a phase shift of 90°. Before stating the algorithm, some properties of the Hilbert transform are examined in the simplest case of a one-dimensional periodic waveform.

Let $F(x)$ be a periodic waveform defined on the interval $T = [-\pi, \pi]$ and suppose that F is square-integrable, so that $F \in L^2(T)$. The function F can thus be expanded as a Fourier series

$$F(x) = \sum a_n \sin(nx + \zeta_n), \quad n \geq 0, \; a_n \geq 0.$$

The Hilbert transform H of F is then simply given by

$$H(x) = \sum a_n \cos(nx + \zeta_n), \quad n > 0.$$

Note that by Parseval's theorem (Titchmarsh, 1948) we know that if F is in $L^2(T)$ then so is H and the norms of F and H are related by

$$\|H\|_2^2 = \|F\|_2^2 - |a_0|^2.$$

Proposition 1. *If F is in $L^2(T)$ then H and F are orthogonal to each other in $L^2(T)$, that is,*

$$\int F(x)H(x)\,dx = 0.$$

Proof. It follows from Parseval's theorem and the fact that the Hilbert transform is a skew-symmetric operator (if H is the Hilbert transform of F, then the Hilbert transform of H is $-F$ (Garnett, 1981)) that

$$\int F(x)H(x)\,dx = -\int H(x)F(x)\,dx = 0. \qquad \square$$

The functions H and F form an orthogonal 2-dimensional basis set in $L^2(T)$ and are thus a quadrature pair. By considering a polar coordinate transformation, the local energy value E is defined by

$$E(x) = F^2(x) + H^2(x),$$

and the argument value Arg is defined by

$$\mathrm{Arg}(x) = \mathrm{Atan}\,2(F(x), H(x)),$$

at each point x. So, for example, a sinewave has a flat energy function (identically equal to 1) and the argument value for each x is just x.

Consider now the components $a_n \sin(nx + \zeta_n)$ of the Fourier transform of F and the corresponding components $a_n \cos(nx + \zeta_n)$ of the Hilbert transform H. Each of these components is a projection, in the 2-dimensional space spanned by F and H, of one of a sequence of functions with amplitude a_n and argument $\phi_n(x) - nx + \zeta_n (\mathrm{mod}\, 2\pi)$ (see Figure 2). This sequence of functions will sum (in L^2) to a function whose modulus is $a(x) = \sqrt{E(x)}$ and whose argument is $\Phi(x) = \mathrm{Arg}(x)$.

For each x, the argument, $\phi_n(x)$, associated with each component, will be distributed with some spread $\sigma(x)$. We say that x is a *point of maximum phase congruency* if $\sigma(x) < \sigma(y)$ for any point y in a small neighbourhood of x. For example, if we define a step edge by

$$S(x) = \begin{cases} 1 & \text{if } 0 \le x \le \pi, \\ -1 & \text{if } -\pi \le x < 0, \end{cases}$$

then the origin is a point of maximum 0°-phase congruency (every component is in 0° phase with $\sigma(0) = 0$). As another example, a pure sinewave has no points of maximum phase congruency.

Because of this representation in the space spanned by the functions H and F and the simple additive properties of vectors we have the following proposition:

Proposition 2. *The maxima of the energy function occur at points of maximum phase congruency.*

Proof. This is clear since the amplitudes a_n are independent of x and hence, for each x, only the phase relationships can effect the length of the resultant vector. $\square$

As discussed in the Introduction, points of maximum phase congruency (e.g., 0° phase congruency at a step edge, or 90° phase congruency at a delta) could be the points where the visual system perceives a feature (Morrone et al., 1986). The

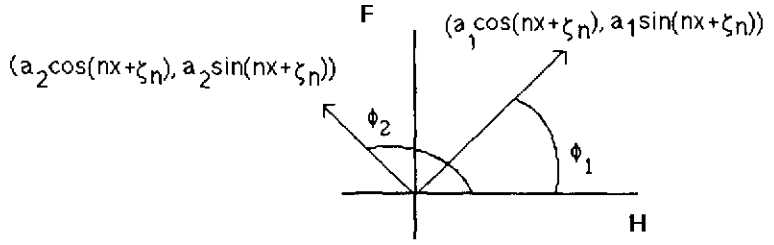

Figure 2.

local energy function, having peaks at these points, could act as a feature detector and suggests the following algorithm:

(a) A feature is detected at a local maximum of E. Let x_0 be a local maximum.

(b) If x_0 is a maximum of H and a zero-crossing of F there is phase congruency of 0°, signalling a positive-going edge; if x_0 is a minimum of H and a zero-crossing of F there is phase congruency of 180°, signalling a negative-going edge. Equivalently, $\mathrm{Arg}(x_0) = 0°$ or 180°.

(c) If x_0 is a maximum of F and a zero-crossing of H there is phase congruency of 90°, signalling a positive delta. If x_0 is a minimum of F and a zero-crossing of H there is a phase congruency of 270°, signalling a negative delta. Equivalently, $\mathrm{Arg}(x_0) = 90°$ or 270°.

(d) All other maxima of the energy function E correspond to other points of phase congruency.

As stated, the algorithm uses the fact that the mean luminance is set to zero. This is equivalent to saying that its Fourier expansion has zero constant term a_0. In the implementation section it is explained how this is obtained by convolving with an appropriate filter.

Figure 3 shows some examples of six different waveforms, their Hilbert transforms, and the energy function E as defined above. Note that the energy function has local maxima at the so-called 'points of interest' for the human visual system; it peaks at points corresponding to the edge in the step function and the all-positive trapezoid, at the points where the Mach bands are perceived at the tangent discontinuities of the trapezoid, and at the peak of the delta function. It is able to locate all the transition points in the staircase function (a difficult function for standard algorithms (Richter and Ullman, 1986)) without marking any false positives. Thus the algorithm will mark as edges the transition points in Figures 3a and 3d, bars at the transition point of the Hilbert transform in Figure 3e, and a different type of feature in Figures 3c and 3f. No features will be marked on the sinewave in Figure 3b. Clearly Mach bands should not be marked as either edges or deltas (Morrone et al. 1986), and neither should the transitions in the staircase. The staircase profile is well known to psychophysicists and illustrates the Chevreul illu-

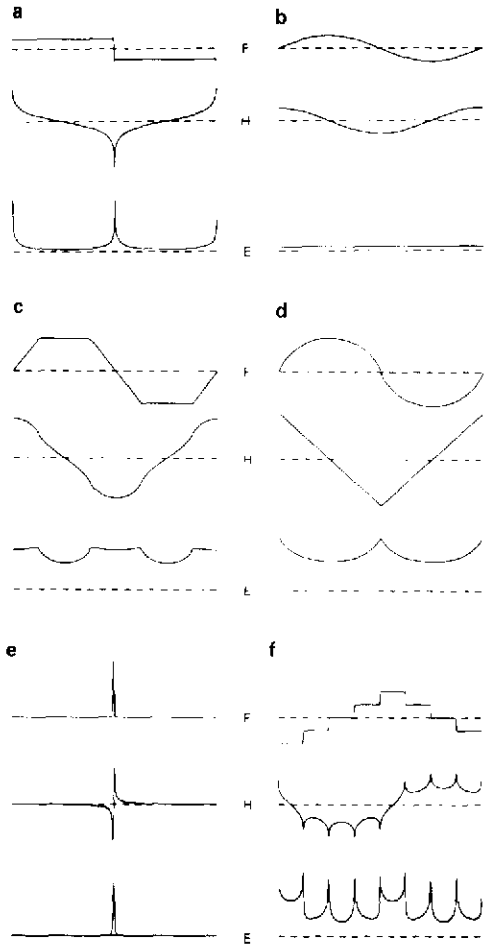

Figure 3. The input waveform (top row), the Hilbert transform (middle row), and the energy function (bottom row) for 6 different waveforms.

(a) A step edge. For each transition the Hilbert transform diverges (behaves like $\log x$ near $x = 0$) and the energy has sharp peaks at these points.

(b) A sinewave. Clearly $\sin^2 x + \cos^2 x = 1$. No feature is detected.

(c) A trapezoidal waveform. Features are detected where Mach bands are perceived. The energy function has local maxima at these points and so they are points of maximum phase congruency. Note that these local maxima do not match peaks or zero-crossings of the function or its Hilbert transform.

(d) An 'all positive trapezoid'. The perceived edge is marked by a maximum in the energy function which corresponds to a zero-crossing of the image and a peak of the Hilbert transform.

(e) A periodic series of delta functions. In this case the Hilbert transform behaves like $1/x$ near $x = 0$ at the delta points. At points of maximum energy the image itself peaks, and the Hilbert transform exhibits a 'zero-crossing'.

(f) A staircase function. All the steps are located and no false positives are detected halfway through the plateau. Note that the maxima of the energy function do not match zero-crossings of the input.

sion (Chevreul, 1890). Each transition of this profile is perceived neither as an edge nor a bar, but rather a combination of the two.

In conclusion, the energy function is used for feature detection in the sense that a feature is simply *defined* as any local maximum of E. The type, sign and contrast of the feature can be determined by the type of phase congruency and the amplitude of the local maxima of the energy function. For the purposes of this paper, a distinction is only made between edges and deltas, and all other phase congruency types are ascribed to a third category.

3. Implementation

Because the Hilbert transform operator is an improper integral, it is not straightforward to calculate it for an arbitrary non-periodic function. To implement the algorithm two functions are constructed, say F_1 and H_1, that are related to each other via the Hilbert transform, with one being as close as possible to the image signal. The functions F_1 and H_1 are obtained by convolving the image signal with two masks, M_F and M_H, one mask being the Hilbert transform of the other.

To determine the shape of the masks M_F and M_H the following two requirements were stipulated:

(a) The function F_1 should be as close as possible to the input waveform. This means that the amplitude spectra of the masks should have a very large bandwidth.

(b) The amplitude spectra of the masks should be exactly equal for all frequencies, and the phase spectra should be constant, 0° for M_F and 90° for M_H.

To avoid any aliasing introduced by sampling, it is important that the spectra have a high frequency limit, reaching zero at the Nyquist frequency. In addition, the attenuation should be smooth and gradual to avoid ringing, which would amplify any noise.

As mentioned before, one requirement of the algorithm is that the mean value of F_1 is zero. In this case, a local maximum of the energy function which is also a zero-crossing of F_1 and a peak of H_1 will uniquely determine an edge. (Recall, the spectrum of the Hilbert transform always has zero mean value, independent of the waveform.) To obtain a zero mean value of F_1, equal low spatial frequency attenuation was introduced for both masks.

Several masks were devised, like the Chebyshev mask, the Hanning mask, the exponential mask etc., satisfying the above constraints (see, for example, Gabel and Roberts, 1980). The results reported in this paper were produced with the masks illustrated in Figure 4. (See caption for details.) All the above masks produced comparable outputs.

To extend the algorithm to a two dimensional image, the input image was convolved with the masks M_F and M_H oriented horizontally and vertically. For each orientation the masks comprised of only one row or one column, saving computational time. After the calculation of the horizontal

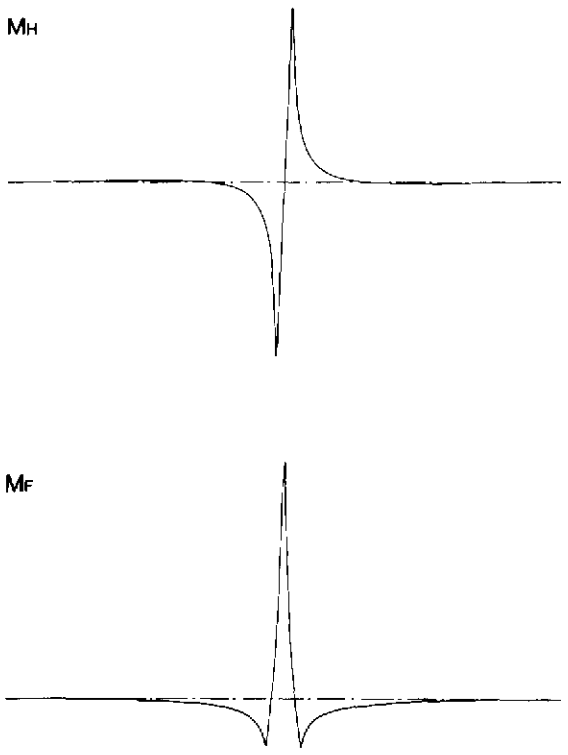

Figure 4. Convolution masks used to produce the results reported in this paper. The two masks have the same amplitude spectra, the even has a zero phase spectrum, the odd has a 90° phase spectrum. The form of the amplitude spectrum is given by the product of the logarithm of the frequency by a Gaussian with σ equal to half of the Nyquist value. The full bandwidth of the filter at half height is about 3 octaves.

and vertical energy, the local maxima along the orientation of the mask were marked. For each horizontal and vertical output, points of local maximum energy were compared with the points of local maxima and minima of the functions F_1 and H_1 to catalogue the type of feature, i.e., an edge, delta, etc.

For all the artificial images (the step edges in noise (Figure 5) and the circle (Figure 6)) no thresholding has been applied. However, for natural images a relative maximum of the energy was marked only if the difference between the value at that point and the value at one of the neighbouring points was greater than some threshold (in these results, the threshold was one). This was necessary since the input recorded by the video camera was quantised in 256 grey levels per pixel, producing a stepwise constant output. The algorithm is sensitive to phase congruency, and detected this step produced by the quantisation. However, no other thresholding technique was used for the natural images.

In summary, the 2-D implementation required the following steps for each orientation:

(i) the input was convolved with the one-dimensional masks M_F and M_H to produce the outputs F_1 and H_1 for the particular orientation.

(ii) the two outputs were squared and summed to produce the energy.

(iii) the local maxima of the energy function along the orientation were marked as features.

(iv) the features were classified as edges or bars depending on the coincidence of the maxima or zero-crossings of the output of the masks along each orientation, as described in Section 2.

The corresponding outputs for each orientation were summed together to produce the final output.

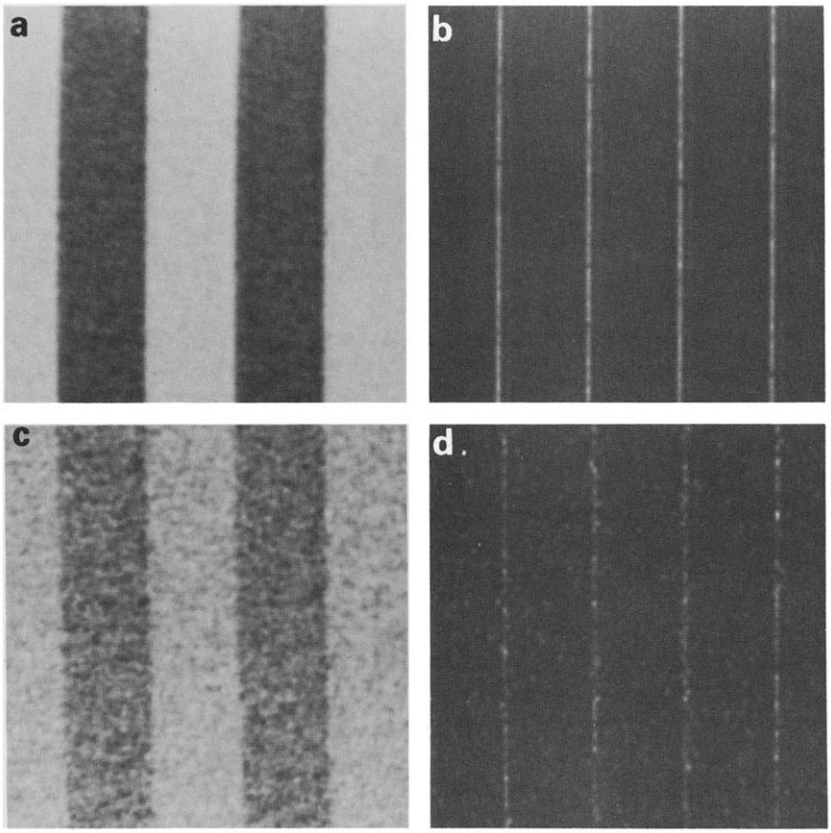

Figure 5. Step edges with varying amounts of noise in (a) and (c), and the corresponding output in (b) and (d). Note that all points of phase congruency, that is, all local maxima of E, have been marked and that no thresholding has been applied. Here, and in all the following figures, the intensity displayed is the square root of the energy function, for graphical representation purposes. In this figure, the picture size is 128×128 pixels.

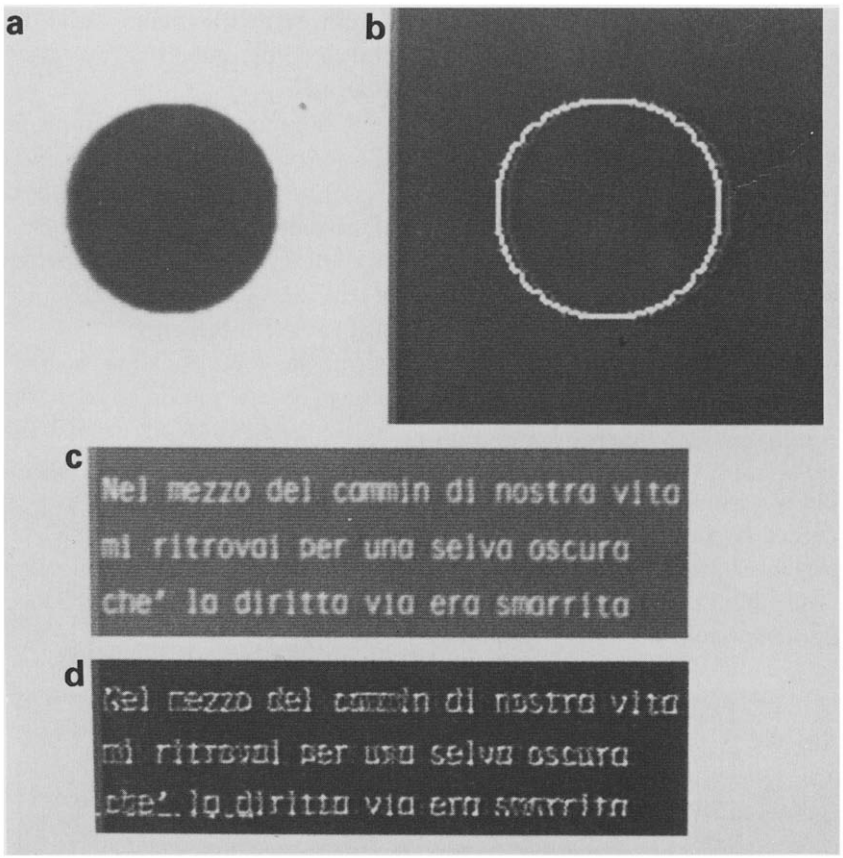

Figure 6. (a) and (b). A disc and its output. Note that the maxima of the energy function closely follows the undersampling of the image. Picture size, 128 × 128 pixels. (c) and (d). Typeface (recorded by video camera) and the corresponding output. Picture size, 110 × 350 pixels.

4. Results

In this section a number of images and the output of the algorithm for each are presented.

Figure 5 shows the response of the algorithm to step edges with low (Figures 5a and 5b) and high (Figures 5c and 5d) amounts of Gaussian noise. Note firstly that the algorithm produces not only good detection, but also good localisation and a single response to a single edge. Even though no thresholding has been applied, the algorithm is fairly robust to noise which, by definition, has random phase information. This would be expected since the algorithm looks for phase congruencies. Phase congruencies may occur randomly in noise, but will do so at isolated points that could easily be eliminated.

Figure 6a depicts a circle at low resolution and Figure 6b shows its output. The response of the algorithm to typeface is shown in Figures 6c and 6d. The output in Fig. 6d is certainly comparable to Canny's bar detection operator, one which has been optimally scaled for detecting a particular typeface. No change of scale was made in producing our results. Notice also that the detector responds to all orientations, including the fine detail of the undersampling of the disc, even though the masks have only two orthogonal orientations. This represents a large computational saving.

Figure 7a shows an image of a coffee mug as seen in diffuse and low lighting with poor contrast. The image contains a number of different features; shadow lines, orientation discontinuities, depth discontinuities and specularities. The maxima of the energy function are depicted in Figure 7b and they easily detect and localize all these features as

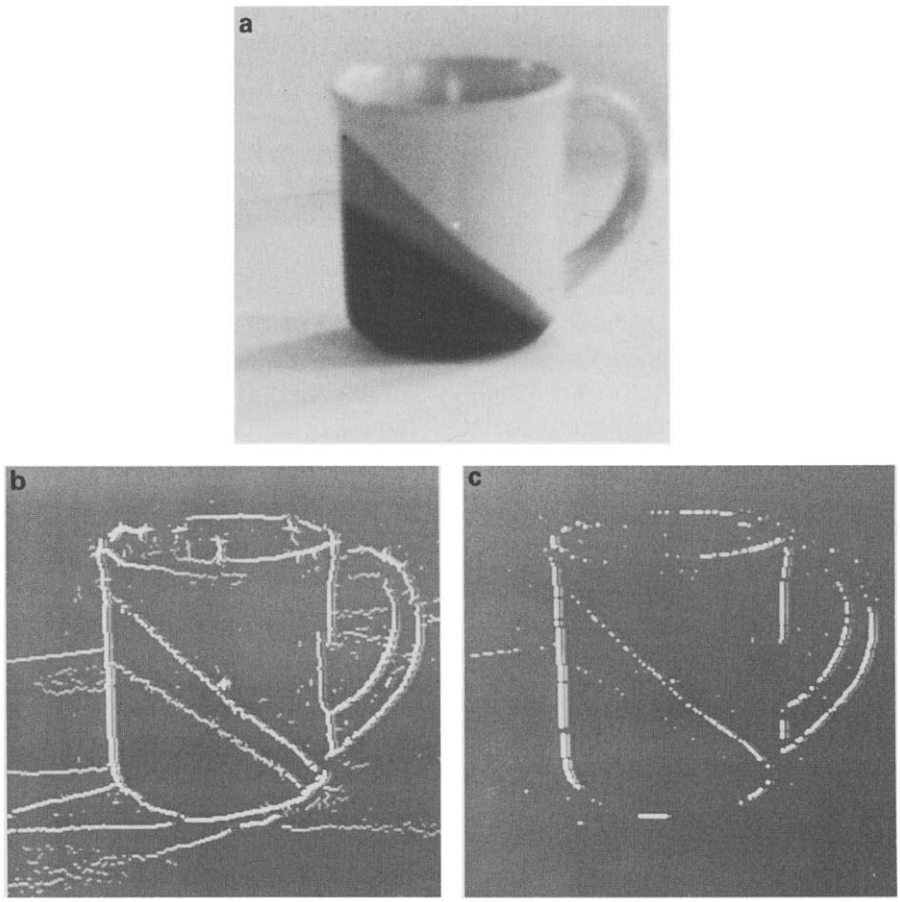

Figure 7. (a) A coffee mug in diffuse lighting. The illumination is low and a lot of noise is present. (b) The points of local maximum energy. Note that all types of features (edges, shadows and specular points) have been detected and localised with a single output. (c) Output corresponding to 0° phase congruency only. The output is incomplete, but no false edges have been marked, like a shadow edge or points of specularity. The noise is considerably reduced from Figure 6(b) since 0° phase congruency in noise is as unlikely as any other type of phase congruency. Picture size, 256 × 256 pixels.

they are perceived by the human visual system. The edge of the mug near the handle is broken, as it is perceived. The rim of the front of the mug is represented by two lines, according to the lighting at each side. Specularity shows up at a number of points. Figure 7c shows the features that correspond to edges as defined by the algorithm. All the 'perceived edges' have been marked. Notice that the shadow edges are no longer present, an important fact for machine vision applications. This is particularly impressive when it is noted that the shadow edges seem stronger than the edge formed by the table at the back of the scene. Yet the table edge is marked and the shadows are eliminated. Note that the same masks have been used for this image and for the typeface in Figure 6c, even though this image contains mostly low frequency information and the typeface contains mostly high frequency information.

5. Discussion

In summary, an efficient algorithm for detecting, localising, and discriminating between various features in an image has been constructed. Since the approach is an integral, rather than a differential one, it is intrinsically more robust to noise and thus offers a number of advantages for machine vision applications. It is very easy to implement since it only needs to consider two orientations and one scale. It could, however, be extended

to encompass several scales, and several orientations.

Other approaches, for example Boie et al. (1986), have recently used a matched filter technique with varying degrees of success. In the first stage of the algorithm presented here the image is filtered with two linear matched filters. The difference from previous work is that here the same matched filters are used for the detection of all feature types. However, to distinguish between different features, as defined in this paper, we need a large bandwidth for both filters. Since this may be difficult to achieve in practice, better results may be obtained by combining the results from both filters over a number of scales. This is currently being investigated and will be reported in a future paper.

Another difference between this method and the previous matched filter techniques is the non-linear energy computations which follow the linear stage. When a non-linear operation is used for detection (the energy function), it is not necessarily true that localisation and detection remain related by an uncertainty principle, as Canny demonstrated. It has been noted (Boie et al., 1986) that the localisation operator is the derivative of the detection operator. The two masks used in this paper are related by the Hilbert transform, an operator closely resembling differentiation (see Garnett, 1981). When an edge is to be detected, the even mask performs better than the odd at localisation. For a delta function this process is reversed. The present algorithm could be improved using the energy function as a feature detector, with the even and odd linear filters performing the localisation. Nevertheless, the results obtained with the energy function performing both the detection and the localisation are already satisfactory for many applications.

Whilst detection and localisation are satisfactory, more work is required to fully understand how each feature (that is, each peak of the energy function) should be classified. For example, a waveform in which the phase of all the components is 45° at some point gives the appearance of having both an edge and a delta at that point (Burr and Morrone, 1987). The definition of an edge in this paper discards such a point, preferring to have an incomplete description of edges, rather than marking false edges.

Recent psychophysical and electrophysiological work has used a similar theory of an energy function to successfully model the performance of the human visual system (Adelson and Bergen, 1985); Morrone et al., 1986; Burr and Morrone, 1987). The fact that the algorithm presented in this paper does not respond to false positives, that is, points of maximum gradient at which humans perceive no edges, further suggests that it may be a good model for the human visual system. One of the major differences between this algorithm and the mechanism possibly used by the human visual system is that only one scale and two orientations are considered. Different scales have advantages for edge detection, as has been noted by many authors (see, for example Hildreth, 1985) and certainly make the system more robust to noise. Nevertheless, the present algorithm is sufficiently robust to allow the advantages to be gained by using multiple scales and orientations to be traded off in favour of simplicity and low computational cost.

We believe that our algorithm offers many advantages over existing algorithms, the major improvements being its robustness to noise, the elimination of false positives, and the identification of different types of features. Further work is required for a full understanding of the type of features that occur in a real-life scene and the role of phase in identifying such features.

Acknowledgements

The authors would like to thank John Ross and David Burr for their help and encouragement. MCM was on leave from the Scuola Normale Superiore, Pisa, and received a National Research Fellowship from the Australian Department of Science. This work has been supported by an ARGS grant.

References

Adelson, E.H. and J.R. Bergen (1985). Spatiotemporal energy

models for the perception of motion. *Optical Society of America* A 2(2), 284–299.

Boie, R.A., I.J. Cox and P. Rehak (1986). On optimum edge recognition using matched filters. *IEEE*, 100–108.

Burr, D.C. and M.C. Morrone (1987). The role of spatial phase in visual analysis. Submitted to *Proc. Royal Soc.*.

Canny, J.F., (1983). Finding edges and lines in images. MIT AI Lab. Tech. Report No. 720.

Chevreul, M.E. (1890). *The Principles of Harmony and Contrast of Colours*. Bell, London, Bohn's Library, translated by Charles Martel.

Gabel, R.A. and R.A. Roberts (1980). *Signals and Linear Systems*. Wiley, Second Edition.

Gabor, D. (1946). Theory of communication. *JIEE Lond.* 93, 429–257.

Garnett, J.B. (1981). *Bounded Analytic Functions*. Academic Press, New York.

Hildreth, E.C. (1985). Edge detection. MIT AI Lab Memo No. 858.

Marr, D. (1980). *Vision*. Freeman, San Francisco.

Marr, D. and E. Hildreth (1980). Theory of edge detection. *Proc. R. Soc. Lond. B* 207, 187–217.

Morrone, M.C., D.C. Burr, J. Ross and R. Owens (1986). Mach bands are phase dependent. *Nature* 324, 250–253.

Ritcher, J. and S. Ullman (1986). Non-linearities in cortical simple cells and the possible detection of zero-crossings. *Biological Cybernetics* 53, 195–202.

Titchmarsh, E.C. (1948). *Introduction to the Theory of Fourier Integrals*. Oxford University Press, Oxford.

Yuille, A.L. and T. Poggio (1985). Fingerprint theorems for zero crossings. *J. Opt. Soc. Am. A* 2(5), 683–692.